Submitted: 31 August, 2022 Accepted: 01 November, 2022 Published: 08 March, 2023 DOI:10.22514/sv.2023.016

Open Access
Signa Vitae

ORIGINAL RESEARCH

Morphometric characteristics of interatrial septum in patients with patent foramen ovale and cryptogenic stroke

Qingyuan Zhang[1,†], Yudong Peng[1,†], Hong Zhang[1], Xiaoling Wan[1], Xiao Liu[1], Wei Xu[1,*]

[1]Department of Ultrasonography, The First Affiliated Hospital of Yangtze University, 434021 Jingzhou, Hubei, China

***Correspondence**
xw_xuwei888@163.com
(Wei Xu)

[†] These authors contributed equally.

Abstract

High-risk morphometric characteristics of patent foramen ovale (PFO), as observed by transesophageal echocardiography (TEE), are associated with cryptogenic stroke (CS) and crucial for selecting optimal treatment. This study aimed to evaluate the pathogenic characteristics and mobility of the interatrial septum (IAS) in patients with PFO and CS. The PFO parameters of 69 patients, including 32 patients with CS and 37 without CS, were assessed using TEE to determine the degree of mobility and pathogenic characteristics. CS patients had more significant IAS mobility, shorter PFO length and thinner septum primum thickness than non-CS patients. Multivariate analysis showed that age, IAS mobility, PFO length and septum primum thickness were independently associated with CS. No correlation was found in the mobility of the middle and edge of the septum primum and septum secundum in both groups of patients. TEE could accurately identify the morphometric characteristics of PFO. CS was associated with PFO characteristics, including age, IAS mobility, PFO length and septum primum thickness.

Keywords

Interatrial septum; Patent foramen ovale; Cryptogenic stroke; Transesophageal echocardiography

1. Introduction

The etiologic significance of cryptogenic stroke (CS) with patent foramen ovale (PFO) has drawn interest from neurologists for decades. Recent research investigating the association between PFO and CS indicated that transcatheter closure of PFO could further reduce stroke recurrence compared with pharmacological treatment [1–3].

PFO is caused by a fusion failure between the septum primum and septum secundum of the foramen ovale, resulting in a flap-like channel between the left and right atria at the fossa ovalis [4]. Recent studies using transesophageal echocardiography (TEE) showed that large PFOs, long-tunnel PFOs, atrial septal aneurysm (ASA), hypermobile interatrial septum (IAS) and prominent Eustachian valve or Chiari network were more frequently found in patients with CS than in those without CS [5, 6]. The pathophysiological mechanism of CS due to various high-risk factors is paradoxical embolism occurring indirectly via an underlying right-to-left shunt pathway [7].

To evaluate CS with TEE, the pathogenicity factors of PFO should be first defined. Although Turc *et al.* [8] reported a higher correlation between ASA and CS compared with other high-risk structures for PFO, the involvement of septum primum and secundum in ASA cannot be ignored.

Several factors influencing the opening of PFO have been identified. Specifically, the size of the PFO opening may vary considerably due to the irregular motion of the primary and secondary septum [9]. However, whether high-risk morphological characteristics of PFO may contribute to CS remains debatable. Some studies reported that PFO with more extended channels could lead to cerebrovascular events [10]; however, other studies found opposing associations, such as short channel PFOs were more likely to allow emboli to pass through the IAS, resulting in cerebrovascular events [11]. Even the definitions of the hypermobility of IAS or an ASA used in some research have been different, thereby emphasizing the lack of agreement on the risks associated with morphologic or functional features of PFO [12].

Previous studies showed that the mobility of IAS was closely related to the opening of PFO and could indirectly increase the risk of CS when using TEE to observe the "curvilinear" movement produced by the septum primum and septum secundum [9, 13]. However, the relationship between CS and the mobility of IAS in patients with PFO remains unclear. Thus, this study aimed to determine the morphometric characteristics of IAS in PFO and its association with CS.

2. Method

2.1 Patient selection

From November 2018 to May 2022, 32 patients with CS (referred to as the "CS group") were diagnosed with PFO following TEE at our institution and were enrolled in this study. CS was diagnosed based on the criteria established by the Trial of Org 10172 in Acute Stroke Treatment or TOAST, which defines CS as an ischemic stroke in patients with no certain source of cardioembolism, no large artery atherosclerosis and no small artery disease, in whom the cause of stroke could not be identified despite extensive evaluation [14]. All patients underwent the following investigations: transthoracic echocardiography, TEE, laboratory tests and 12-lead electrocardiogram monitoring. Patients diagnosed with atrial septal defects or underwent any IAS interventions were excluded from this study, as well as those with heart valve disease, myocardial infarction, infective endocarditis, cardiac mucinous tumors, or intracardiac thrombosis.

The control group comprised 36 patients without any history of stroke and cardiac disease who underwent TEE for other clinical reasons and were diagnosed with PFO.

The following risk factors were considered for CS: ever smoker, diabetes mellitus, arterial hypertension, hyperlipidemia and D-dimer abnormality.

2.2 Echocardiography

TEE was conducted using Philips EPIQ 7C (Philips Ultrasound Inc, Bothell, USA) with the X7-2T probe or Philips iE33 (Philips Ultrasound Inc, Bothell, USA) with the S7-2omni probe. Oropharyngeal anesthesia was performed using dyclonine hydrochloride plasma to reduce pain. The blood pressure, heart rate and electrocardiogram of the patients were monitored throughout the examination. Following thorough and systematic evaluations of IAS and PFO, the septum was examined in multiple median esophageal views by an experienced physician using optimized two-dimensional images and color Doppler. Using TEE, the presence of PFO was confirmed by direct observation of the gap between the septum primum and septum secundum on Color Doppler imaging or by injecting oscillating saline (0.9% saline, 1 mL patient blood, 1 mL air) into the median cubital vein in the resting state when the channel was directly visible by Color Doppler imaging (**Supplemental Fig. 1A**) or when microbubbles entered the left atrium from the right atrium within three cardiac cycles in right atrial visualization after injecting oscillating saline (**Supplemental Fig. 1B**).

Post-processing and image evaluation were performed on an imaging workstation using the RadiAnt DICOM Viewer Version 2021.1 (Medixant, Poznan, Poland). All images were reviewed and independently evaluated by two experienced investigators who analyzed all TEE datasets. A blinded approach was employed to render the presence or absence of stroke invisible to the investigators. The morphometric characteristics of PFO were also evaluated.

2.3 Image interpretation

The mobility and anatomy of the IAS were measured with TEE. IAS mobility was defined as the excursion distance of the IAS in a single cardiac cycle recorded during consecutive scans (Fig. 1A2) [15, 16]. Measurements were made at four levels, namely, the lower edge and midpoint of the septum primum and the upper edge and midpoint of the septum secundum (Fig. 1A4). The PFO length was defined as the maximum visible area of overlap between the septum primum and septum secundum (Fig. 1B1–B2). The PFO height was defined as the maximum distance between the septum primum and septum secundum (Fig. 1C1–C2). The maximum thicknesses of the septum primum and septum secundum were measured using the bicaval view (Fig. 1D1–D2). The distance from the opening of the right atrial surface of the PFO to the root of the aorta (septum secundum height; Fig. 1E1–E2) was measured in aortic short-axis views. The angle between inferior vena cava (IVC) and PFO was measured on the imaging plane showing the IVC and IAS (Fig. 1F1–F2).

To assess the reproducibility and accuracy of the study results, two investigators experienced in TTE image interpretation and blinded to patient information and examination findings analyzed all images independently for determining interobserver variability. Within one week of the initial assessment, 20 randomly selected patients were re-assessed by the same investigators in a blinded fashion to calculate intraobserver variability.

2.4 Statistical analysis

Statistical analyses were performed using the software MedCalc® Statistical Software version 20.114 (MedCalc Software Ltd, Ostend, Belgium) and the language R version 4.0.2 (R Foundation for Statistical Computing, Vienna, Austria). The values of continuous variables are expressed as mean $\pm$ standard deviation. Categorical variables are expressed as percentages, and comparisons were performed using the chi-squared test or Fisher's exact test. The Shapiro-Wilk test was used to determine whether continuous variables followed a normal distribution; if so, the parameters between the two groups were compared using an independent t-test. If the continuous values did not follow a normal distribution, they were analyzed using the Mann-Whitney U test and expressed as the median (50th) and interquartile range (25th and 75th). Univariate logistic regression was performed, followed by multivariate logistic regression (with backward likelihood ratio statistic), with CS as the dependent variable. Patient characteristics, mobility and anatomical feature parameters of PFO were preselected independent variables to determine the independent risk factors of CS. The strength of association was measured using $p < 0.05$ and validated with the odds ratio (OR) and 95% compliance.

Intragroup correlation coefficients were calculated. Interobserver agreement was plotted using the Bland-Altman method to compare the measurements of the two independent investigators. Interobserver (based on the entire cohort) and intraobserver (based on 20 cases from the cohort) variability were assessed using intragroup correlation coefficients. An intraclass correlation coefficient of 0.7 to 0.8 indicated strong agreement, whereas a value > 0.8 indicated excellent agreement.

Receiver operating characteristic (ROC) curve analysis was performed to obtain area under curve (AUC) and investigate the predictive value of morphologic parameters of PFO in

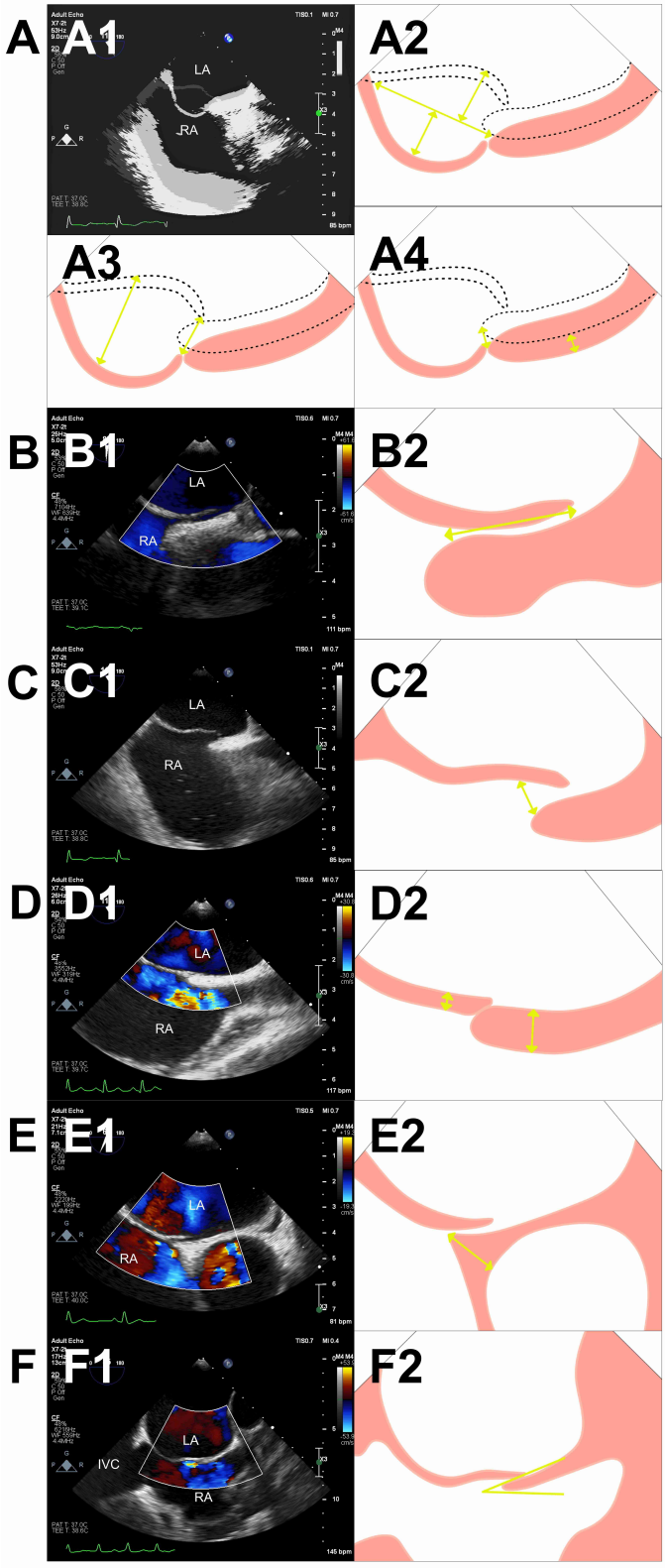

FIGURE 1. Measurement of the morphometric characteristics of IAS. Overlapping of two images upon septum excursion to the left and right atria in a cardiac cycle (A1) and the measurement of the IAS mobility (A2). Measurement of the midpoint and lower-edge mobility of the septum primum (A3) and the midpoint and upper-edge mobility of the septum secundum (A4) in a single cardiac cycle recorded during consecutive scans. The PFO length was defined as the maximum visible area of overlap between the septum primum and septum secundum (B1–2). The PFO height was defined as the maximum distance between the septum primum and septum secundum (C1–2). The maximum thicknesses of the septum primum and septum secundum were measured in the bicaval view (D1–2). Measurement of the septum secundum height measured in the short axis of the aorta (E1–2). Measurement of the angle between the IVC and PFO (F1–2). Abbreviations: LA, Left atrium; RA, Right atrium; IVC, inferior vena cava.

detecting CS. The Youden index was used to identify the optimal cutoff value that maximized the difference between the true positive and false positive rates for all possible cutoff values.

3. Results

The comparison of baseline characteristics between the CS (n = 32) and control group (n = 36) patients is shown in Table 1. The results showed that patients from the CS group were older, more hypertensive and had significantly higher Body Mass Index (BMI) than those from the control group.

The morphometric characteristics of the IAS between the two groups of patients are presented in Table 2. We found that the CS group had significantly greater IAS mobility, shorter PFO length and thinner septum primum thickness than the control group. However, no significant difference in the mobility of each part of the septum primum and septum secundum (midpoint and edges) and thickness of the septum secundum was found between the two groups. In addition, no difference in PFO height and no significant differences in the angle between the inferior vena cava and the PFO were found between the two groups.

Univariate analysis showed that age, BMI, arterial hypertension, IAS mobility, PFO length and septum primum thickness were identified as significant indicators associated with CS, and multivariable analyses confirmed that age, IAS mobility, PFO length and septum primum thickness were independently associated with increased CS risk (Table 3).

Subsequent analyses were performed using ROC curves to determine the cutoff values by selecting the four independently correlated features identified in the multifactorial regression analysis and for determining the thresholds that could indicate significant change points for quantitative variables (Fig. 2). The results showed that characteristics associated with PFO patients for which the risk of CS might be significantly increased included age $\geq$41.5 years, IAS mobility $\geq$9.58 mm, PFO length $\leq$10.25 mm and septum primum thickness $\leq$1.57 mm. To predict the association between PFO patients and CS, the predictive ability of the variable age (cutoff value = 41.5 years) had a sensitivity of 38.9% and a specificity of 87.5% (AUC = 0.658, CI = 0.528–0.789). The cutoff value for IAS mobility was 9.58 mm, with a sensitivity of 65.6% and a specificity of 69.4% (AUC = 0.691, CI = 0.562–0.819). A PFO length of 10.25 mm demonstrated a sensitivity of 59.4% and a specificity of 69.4% for diagnosing CS (AUC = 0.646, CI = 0.514–0.778) and the septum primum thickness $\leq$1.565 mm had a sensitivity of 62.5% and a specificity of 66.7% (AUC = 0.662, CI = 0.532–0.793) for predicting CS. The accuracy of the combination of PFO length, IAS mobility and septum primum thickness demonstrated a certain degree of accuracy in diagnosing CS (AUC = 0.773, CI = 0.661–0.886, sensitivity = 68.8%, specificity = 80.6). However, the combination of age, PFO length, IAS mobility and septum primum thickness demonstrated a greater degree of accuracy for CS diagnosis, with a sensitivity of 86.1% and a specificity of 71.9% (AUC = 0.861, CI = 0.776–0.947) (Table 4).

Lastly, intraobserver and interobserver variability assessments were performed to assess the credibility of our findings. The results, based on the Bland-Altman plots, showed good agreement in intraobserver and interobserver variability for all PFO morphometric parameters (**Supplementary Table 1** and **Supplementary Fig. 2**).

4. Discussion

This study compared the anatomical and mobility parameters of IAS between the CS and control group with PFO to identify PFO features associated with high stroke risks, based on which age, IAS mobility, PFO length and septum primum thickness were found to be independently correlated with CS. However, no correlation was found between the mobility of the septum primum and secundum with CS.

Transcatheter closure of PFO was recently reported as an effective treatment for CS [1–3]. Thus, proper evaluation of PFO patients is needed to accurately identify those who would benefit most from this intervention [6]. Additionally, stratified diagnosis for patients is important, including the choice of subsequent treatment modalities and surgical procedures, which directly correlates with the pathogenic characteristic of the PFO formed by IAS [17]. TEE is recognized as the gold standard for evaluating the pathogenic characteristics of PFO [18, 19].

Nakayama *et al.* [10] established a scoring system by comparing the anatomical morphology and function of PFO in CS patients with a control group. The aforementioned system considered the following as high-risk anatomical factors with a score of 1: long-tunnel PFO, hypermobile IAS, prominent Eustachian valve or Chiari network, larger shunt during Valsalva maneuver, and low-angle PFO; based on which patients with a PFO score $\geq$2 would be considered as high-risk and could be recommended for occlusion, with a specificity and sensitivity for CS of 81% and 91%. The PFO-Associated Stroke Causal Likelihood (PASCAL) Classification System combines the Risk of Paradoxical Embolism score with a large number of shunts or ASA as high-risk structures. It also calculates the probability of a causal relationship between PFO patients and CS based on pathological and epidemiologic factors [20].

In 1877, Cohnheim *et al.* [21] proposed the occurrence of possible paradoxical embolism. A series of embolic events arise from emboli of the venous system reaching systemic circulation via shunts in the heart or lungs. High-risk factors of PFO indirectly lead to conditions conducive to paradoxical embolism by increasing the degree of blood flow through the PFO and increasing the chances of PFO opening [22]. Other causes of paradoxical embolism in the PFO can be summarized as follows. (i) local thrombosis exists within the PFO channel or local blood stasis at the left side of the IAS, or thrombus formation occurs within the atrial septal aneurysms concomitant with the PFO [23]; (ii) left atrial electrical activity may be altered in the presence of a PFO, further increasing the risk for stroke; (iii) IAS stretching induced by atrial septal aberrations (*i.e.*, large PFO channel, ASA) can modify atrial depolarization, activating an arrhythmogenic substrate; and (iv) atrial cardiomyopathy, the state of left atrial wall dysfunction, is associated with increased prevalence of atrial fibrillation, atrial thrombi and overall thromboembolic risk [24, 25]. In our study, there were no patients with ASA,

TABLE 1. Baseline characteristics of the patients included in this study.

Parameters	Cryptogenic stroke group (n = 32)	Control group (n = 36)	*p*
Male gender, n(%)	21 (65.6)	17 (30.6)	0.127
Median age, years (IQR)	57.5 (48.0–66.5)	52 (36.3–61.5)	0.025
Body Mass Index, kg/m^2 (IQR)	24.9 (21.0–28.8)	23 (18.7–27.1)	0.045
Ever smoker, n(%)	12 (37.5)	8 (22.2)	0.168
Diabetes mellitus, n(%)	4 (12.5)	6 (16.7)	0.739
Arterial hypertension, n(%)	16 (50.0)	7 (19.4)	0.008
Hyperlipidemia, n(%)	10 (31.3)	8 (22.2)	0.400
D-Dimer abnormality, n(%)	3 (9.4)	4 (11.1)	1.000

Abbreviations: IQR, inter quartile range.

TABLE 2. Morphometric characteristics of IAS with comparison between the CS group and the control group.

Parameters	Cryptogenic stroke group (n = 32)	Control group (n = 36)	*p*
Mobility of the midpoint of the septum primum, mm	9.7 (6.9–12.5)	9.0 (6.5–11.4)	0.269
Mobility of the lower edge of the septum primum, mm	10.0 (7.2–12.8)	9.4 (6.9–11.8)	0.328
Mobility of the upper edge of the septum secundum, mm	9.3 (6.9–11.8)	8.8 (6.5–11.1)	0.383
Mobility of the midpoint of the septum secundum, mm	8.8 (6.4–11.1)	8.3 (6.3–10.3)	0.384
IAS mobility, mm	10.5 (8.8–11.2)	8.8 (8.0–10.3)	0.007
PFO length, mm	10.3 (7.4–13.3)	12.2 (8.6–15.8)	0.023
PFO height, mm	1.2 (1.0–1.6)	1.4 (1.0–1.7)	0.499
Angle between IVC and PFO, degrees	22.9 (16.7–29.2)	23.9 (16.9–30.8)	0.578
Septum primum thickness, mm	1.5 (1.1–1.8)	1.7 (1.3–2.1)	0.018
Septum secundum thickness, mm	4.0 (3.5–5.2)	4.1 (3.1–5.3)	0.623
Septum secundum height, mm	13.6 (10.2–17.1)	13.9 (10.6–17.3)	0.710

If the continuous variable did not follow a normal distribution, they were expressed as the median (50th) and interquartile range (25th and 75th).
Abbreviations: IAS, interatrial septum; CS, cryptogenic stroke; PFO, patent foramen ovale; IVC, inferior vena cava.

prominent Eustachian valves and Chiari network.

This study confirms the correlation of IAS mobility with CS, which was consistent with previous findings. Our study was prompted by the daily observation that septum mobility did not have a linear point-to-point relationship, but instead, each component of the septum primum and septum secundum had a distinct "curvilinear" motion [9]. However, this study found neither a connection between the different degrees of mobility and CS of the primary and secondary septa nor a pattern among all mobility parameters. Two possible reasons could explain this observation: (i) the sample size was too small, which needs to be increased in subsequent studies, and (ii) the involvement of too many influencing factors among the mobility levels. Thus, reducing the number of mobility level indicators with insignificant changes could demonstrate the correlations between several indicators.

This study also found a correlation between thinner septum primum thickness and CS. This correlation could be attributed to the important role of the mobility of the soft septal rim and the overlapping structure of the septum secundum in determining the size of the PFO opening. The presence of a thinner septum also suggests increased septum mobility. A thin primary septum indicates that the elastic fiber component dominates its structure, thus demonstrating increased mobility. Meanwhile, a larger septum thickness indicates the presence of muscle fibers, reducing the flexibility of the septum [26]. Accordingly, the septum secundum height affects PFO tunneling, with shorter heights failing to support the free wall adequately [5].

The low angle of the inferior vena cava to the PFO is also considered a high-risk factor, similar to the prominent Eustachian valve or Chiari network, which preferentially directs the inferior vena cava blood flow to the atrial septum and the PFO orifice [8, 10]. Most patients with small angles in our study involved patients without CS, and no correlation was found between them.

The role of PFO length in patients with CS is controversial. A previous study reported that altered blood flow velocity in long tunnels could be favorable sites for thrombus survival [10]. Our results support the opposite, whereby shorter tunnel lengths were present in more patients with CS because a shorter channel distance could lead to lesser resistance for embolism

TABLE 3. Univariate and multivariate analyses of risk factors for CS.

	Univariate analysis		Multivariate analysis	
Parameters	Odds ratio (95% CI)	*p*	Odds ratio (95% CI)	*p*
Gender	0.469 (0.176–1.249)	0.130		
Age	1.044 (1.006–1.084)	0.025	1.079 (1.019–1.134)	0.009
Body Mass Index	1.132 (1.000–1.281)	0.050		
Ever smoker	2.100 (0.726–6.078)	0.171		
Diabetes mellitus	0.714 (0.182–2.800)	0.629		
Arterial hypertension	4.143 (1.410–12.171)	0.010	4.849 (0.927–25.353)	0.061
Hyperlipidemia	1.591 (0.538–4.706)	0.401		
D-Dimer abnormality	0.828 (0.171–4.018)	0.814		
Mobility of the midpoint of the septum primum	1.111 (0.923–1.388)	0.266		
Mobility of the lower edge of the septum primum	1.098 (0.912–1.322)	0.324		
Mobility of the upper edge of the septum secundum	1.097 (0.893–1.347)	0.377		
Mobility of the midpoint of the septum secundum	1.106 (0.884–1.384)	0.379		
IAS mobility	1.445 (1.066–1.958)	0.018	1.736 (1.123–2.683)	0.013
PFO length	0.837 (0.714–0.981)	0.028	0.665 (0.509–0.868)	0.003
PFO height	0.809 (0.299–2.189)	0.676		
Angle between IVC and PFO	0.979 (0.910–1.053)	0.572		
Septum primum thickness	0.226 (0.063–0.815)	0.023	0.098 (0.014–0.666)	0.018
Septum secundum thickness	1.081 (0.721–1.620)	0.707		
Septum secundum height	0.973 (0.844–1.122)	0.706		

Multivariate analysis with backward likelihood ratio statistics
Abbreviations: CS, cryptogenic stroke; CI, confidence interval; PFO, patent foramen ovale; IAS, interatrial septum; IVC, inferior vena cava.

TABLE 4. Receiver operating characteristic curve for predicting CS.

Predictive variable	AUC	Odds ratio (95% CI)	*p*	Cut-off value	Sensitivity	Specificity	Positive predictive value	Negative predictive value	Yoden index
Age	0.658	0.528–0.789	0.025	41.500	0.389	0.875	0.778	0.560	0.264
IAS mobility	0.691	0.562–0.819	0.007	9.580	0.656	0.694	0.656	0.694	0.351
PFO length	0.646	0.514–0.778	0.039	10.250	0.594	0.694	0.633	0.658	0.288
Septum primum thickness	0.662	0.532–0.793	0.022	1.565	0.625	0.667	0.625	0.667	0.292
IAS mobility + PFO length + Septum primum thickness	0.773	0.661–0.886	0.000	0.517	0.688	0.806	0.759	0.744	0.493
Age + IAS mobility + PFO length + Septum primum thickness	0.861	0.776–0.947	0.000	0.572	0.861	0.719	0.775	0.821	0.580

Abbreviations: CS, cryptogenic stroke; PFO, patent foramen ovale; IAS, interatrial septum; AUC, area under curve; CI, confidence interval.

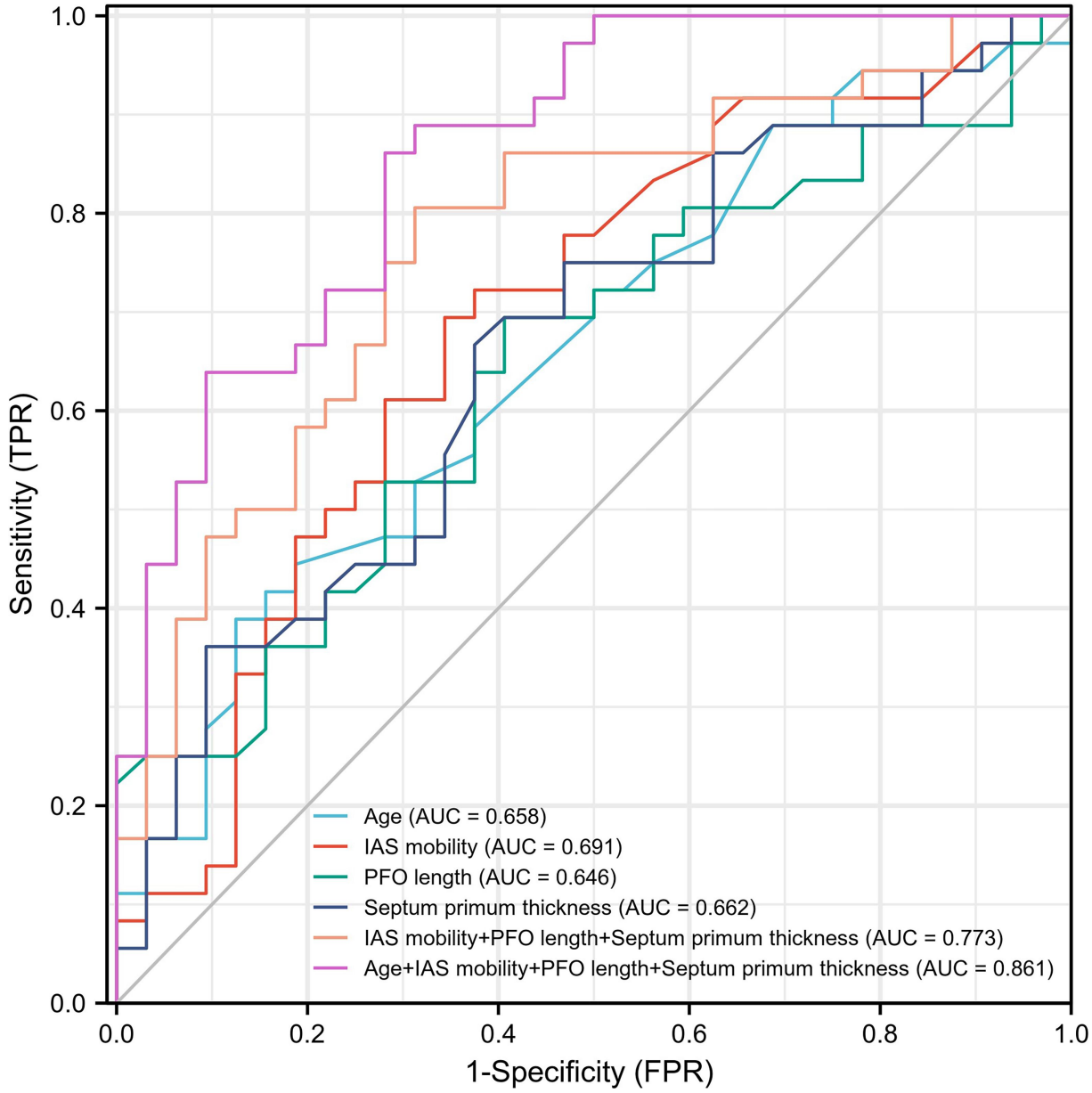

FIGURE 2. Receiver operating characteristic curve of age, IAS mobility, PFO length and septum primum thickness for detecting CS. Abbreviations: IAS, interatrial septum; PFO, patent foramen ovale; CS, cryptogenic stroke; AUC, area under curve; TPR, true positive rate; FPR, false positive rate.

[11]. Therefore, further studies need to elucidate the relationship between PFO length and CS and determine the underlying mechanism.

Prior studies mainly concentrated on patients aged 18–60 years. However, the increased risk of paradoxical embolism due to increased incidence of venous thromboembolism [27], the altered hemodynamics of right-to-left shunts in older patients [28] and the increasing diameter of the PFO with age should not be neglected [29]. Our study also observed an association between age and CS in patients with PFO.

This study had several limitations that should be described. First, unlike most studies that focused on patients aged 18–60 years, we selected patients aged 19–76 years, although the sample size was small. Thus, this study may yield experimental results inconsistent with those obtained from related studies. Second, one of the most influential factors was the effect of respiratory motion, which we tried to avoid by using two independent investigators and strictly the same cardiac cycle, with good reproducibility and accuracy.

5. Conclusions

In this current research, the morphometric characteristics of PFO were evaluated by TEE, including the mobility and anatomical structures of the interatrial septum. The results identified new indicators of septum primum and septum secundum mobility and attempted to exploit its association with CS. Age, IAS mobility, PFO length and septum primum thickness in PFO patients were independently associated with CS. TEE provided a comprehensive observation of the mobility and anatomical structures of PFO and was essential in assessing its association with CS. Our study provides

exciting insights into the pathogenic factors of PFO, focusing on the mobility of the septum primum and septum secundum. Although the mobility indicators of septum primum and secundum proposed for the first time in this study suggest new directions into high-risk factors for PFO, these findings should still be validated in future studies.

AVAILABILITY OF DATA AND MATERIALS

The data presented in this study are available on reasonable request from the corresponding author.

AUTHOR CONTRIBUTIONS

QYZ and YDP—designed the study, completed the experiment and supervised the data collection, HZ—analyzed the data, interpreted the data, XLW, XL and WX—prepare the manuscript for publication and reviewed the draft of the manuscript. All authors have read and approved the manuscript.

ETHICS APPROVAL AND CONSENT TO PARTICIPATE

Ethical approval was obtained from the Ethics Committee of the First People's Hospital of Jingzhou (committee's reference number: LL202280). Written informed consent was obtained from a legally authorized representative(s) for anonymized patient information to be published in this article.

ACKNOWLEDGMENT

Thanks to all the peer reviewers for their opinions and suggestions.

FUNDING

This research received no external funding.

CONFLICT OF INTEREST

The authors declare no conflict of interest.

SUPPLEMENTARY MATERIAL

Supplementary material associated with this article can be found, in the online version, at https://oss.signavitae.com/mre-signavitae/article/1633289830847660032/attachment/Supplementary%20material.docx.

REFERENCES

[1] Søndergaard L, Kasner SE, Rhodes JF, Andersen G, Iversen HK, Nielsen-Kudsk JE, *et al*. Patent foramen ovale closure or antiplatelet therapy for cryptogenic stroke. The New England Journal of Medicine. 2017; 377: 1033–1042.

[2] Saver JL, Carroll JD, Thaler DE, Smalling RW, MacDonald LA, Marks DS, *et al*. Long-term outcomes of patent foramen ovale closure or medical therapy after stroke. The New England Journal of Medicine. 2017; 377: 1022–1032.

[3] Mas JL, Derumeaux G, Guillon B, Massardier E, Hosseini H, Mechtouff L, *et al*. Patent foramen ovale closure or anticoagulation *vs.* antiplatelets after stroke. The New England Journal of Medicine. 2017; 377: 1011–1021.

[4] Webster MW, Chancellor AM, Smith HJ, Swift DL, Sharpe DN, Bass NM, *et al*. Patent foramen ovale in young stroke patients. Lancet. 1988; 2: 11–12.

[5] Hołda M, Koziej M. Morphometric features of patent foramen ovale as a risk factor of cerebrovascular accidents: a systematic review and meta-analysis. Cerebrovascular Diseases. 2020; 49: 1–9.

[6] Lee PH, Song JK, Kim JS, Heo R, Lee S, Kim DH, *et al*. Cryptogenic stroke and high-risk patent foramen ovale: The DEFENSE-PFO Trial. Journal of the American College of Cardiology. 2018; 71: 2335–2342.

[7] Windecker S, Stortecky S, Meier B. Paradoxical embolism. Journal of the American College of Cardiology. 2014; 64: 403–415.

[8] Turc G, Lee J, Brochet E, Kim JS, Song J, Mas J. Atrial septal aneurysm, shunt size, and recurrent stroke risk in patients with patent foramen ovale. Journal of the American College of Cardiology. 2020; 75: 2312–2320.

[9] Zhu Y, Zhang J, Huang B, Liu Y, Deng Y, Weng Y, *et al*. Impact of patent foramen ovale anatomic features on right-to-left shunt in patients with cryptogenic stroke. Ultrasound in Medicine & Biology. 2021; 47: 1289–1298.

[10] Nakayama R, Takaya Y, Akagi T, Watanabe N, Ikeda M, Nakagawa K, *et al*. Identification of high-risk patent foramen ovale associated with cryptogenic stroke: development of a scoring system. Journal of the American Society of Echocardiography. 2019; 32: 811–816.

[11] Natanzon A, Goldman ME. Patent foramen ovale: anatomy versus pathophysiology—which determines stroke risk? Journal of the American Society of Echocardiography. 2003; 16: 71–76.

[12] Ahmad Y, Howard JP, Arnold A, Shin MS, Cook C, Petraco R, *et al*. Patent foramen ovale closure *vs.* medical therapy for cryptogenic stroke: a meta-analysis of randomized controlled trials. European Heart Journal. 2018; 39: 1638–1649.

[13] Homma S, Messé SR, Rundek T, Sun Y, Franke J, Davidson K, *et al*. Patent foramen ovale. Nature Reviews Disease Primers. 2016; 2: 15086.

[14] Adams HP, Bendixen BH, Kappelle LJ, Biller J, Love BB, Gordon DL, *et al*. Classification of subtype of acute ischemic stroke. Definitions for use in a multicenter clinical trial. TOAST. Trial of Org 10172 in Acute Stroke Treatment. Stroke. 1993; 24: 35–41.

[15] Akhondi A, Gevorgyan R, Tseng C, Slavin L, Dao C, Liebeskind DS, *et al*. The association of patent foramen ovale morphology and stroke size in patients with paradoxical embolism. Circulation: Cardiovascular Interventions. 2010; 3: 506–510.

[16] Mügge A, Daniel WG, Angermann C, Spes C, Khandheria BK, Kronzon I, *et al*. Atrial septal aneurysm in adult patients. A multicenter study using transthoracic and transesophageal echocardiography. Circulation. 1995; 91: 2785–2792.

[17] Musto C, Cifarelli A, Dipasquale F, Chin D, Nazzaro MS, Stio RE, *et al*. A comparison between gore cardioform and amplatzer septal occluder for percutaneous closure of patent foramen ovale associated with atrial septal aneurysm: clinical and echocardiographic outcomes. The Journal of Invasive Cardiology. 2021; 33: E857–E862.

[18] de Belder MA, Tourikis L, Leech G, Camm AJ. Risk of patent foramen ovale for thromboembolic events in all age groups. The American Journal of Cardiology. 1992; 69: 1316–1320.

[19] Pearson AC, Labovitz AJ, Tatineni S, Gomez CR. Superiority of transesophageal echocardiography in detecting cardiac source of embolism in patients with cerebral ischemia of uncertain etiology. Journal of the American College of Cardiology. 1991; 17: 66–72.

[20] Kent DM, Saver JL, Kasner SE, Nelson J, Carroll JD, Chatellier G, *et al*. Heterogeneity of treatment effects in an analysis of pooled individual patient data from randomized trials of device closure of patent foramen ovale after stroke. JAMA. 2021; 326: 2277–2286.

[21] Cohnheim JF. Thrombose und Embolie. In: Vorlesungenüber Allgemeine pathologie. Berlin: Hirschwald. 1877; 1: 134.

[22] Rigatelli G, Dell'Avvocata F, Cardaioli P, Giordan M, Braggion G, Aggio S, *et al*. Permanent right-to-left shunt is the key factor in managing patent foramen ovale. Journal of the American College of Cardiology. 2011; 58: 2257–2261.

[23] Yan C, Li H. Preliminary investigation of in situ thrombus within patent foramen ovale in patients with and without stroke. JAMA. 2021; 325: 2116–2118.

[24] Bang OY, Lee MJ, Ryoo S, Kim SJ, Kim JW. Patent foramen ovale and stroke-current status. Journal of Stroke. 2015; 17: 229–237.

[25] Rigatelli G, Aggio S, Cardaioli P, Braggion G, Giordan M, Dell'avvocata F, *et al*. Left atrial dysfunction in patients with patent foramen ovale and atrial septal aneurysm: an alternative concurrent mechanism for arterial embolism? JACC: Cardiovascular Interventions. 2009; 2: 655–662.

[26] Klimek-Piotrowska W, Hołda MK, Koziej M, Piątek K, Hołda J. Anatomy of the true interatrial septum for transseptal access to the left atrium. Annals of Anatomy. 2016; 205: 60–64.

[27] Anderson FA Jr, Wheeler HB, Goldberg RJ, Hosmer DW, Patwardhan NA, Jovanovic B, *et al*. A population-based perspective of the hospital incidence and case-fatality rates of deep vein thrombosis and pulmonary embolism. The Worcester DVT Study. Archives of Internal Medicine. 1991; 151: 933–938.

[28] Homma S, DiTullio MR, Sacco RL, Sciacca RR, Mohr JP. Age as a determinant of adverse events in medically treated cryptogenic stroke patients with patent foramen ovale. Stroke. 2004; 35: 2145–2149.

[29] Hagen PT, Scholz DG, Edwards WD. Incidence and size of patent foramen ovale during the first 10 decades of life: an autopsy study of 965 normal hearts. Mayo Clinic Proceedings. 1984; 59: 17–20.

How to cite this article: Qingyuan Zhang, Yudong Peng, Hong Zhang, Xiaoling Wan, Xiao Liu, Wei Xu. Morphometric characteristics of interatrial septum in patients with patent foramen ovale and cryptogenic stroke. Signa Vitae. 2023; 19(2): 82-90. doi: 10.22514/sv.2023.016.